2016

Experimentally Validated Model of Transient Heat Transfer between a Magnetocaloric Packed Particle Bed and Stagnant Interstitial Fluid

Michael Goodman Schroeder
General Electric, United States of America / University of Louisville, United States of America, michael.schroeder2@ge.com

Ellen Brehob
University of Louisville, United States of America, ellen.brehob@louisville.edu

Michael Benedict
michael.benedict@ge.com

Experimentally Validated Model of Transient Heat Transfer between a Magnetocaloric Packed Particle Bed and Stagnant Interstitial Fluid

Michael Goodman Schroeder [1,2,*], Ellen Brehob [2], Michael Benedict [1,3]
1: General Electric Appliance Division, Louisville, KY, USA
2: University of Louisville Mechanical Engineering Department, Louisville, KY, USA
3: University of Florida Mechanical Engineering Department, Gainesville, FL, USA

ABSTRACT

Typical simulations of packed bed active magnetocaloric regenerators rely on correlations of Nusselt number as a function of Reynolds number. These models are well understood for large ranges of Reynolds number, but experimental data is lacking as Reynolds number approaches zero. Within a typical magnetocaloric refrigeration cycle a zero fluid velocity or dwell condition is present. When a cycle is heat transfer rate limited, heat transferred during dwell represents a significant portion of total heat transferred for a full cycle and must be accurately represented. An experiment was performed in order to validate a basic heat transfer model between a packed magnetocaloric particle bed and stagnant interstitial fluid. A second experiment was performed to measure average particle sphericity using a modified version of the Ergun equation, such that both particle size and sphericity are known for use in the heat transfer model. Finally, a correction factor was applied to the model to reduce error when compared with experimental results.

1. INTRODUCTION

The field of magnetocaloric refrigeration has gained momentum in the last 40 years, and continues to grow (Gschneider Jr. and Pecharsky, 2008). The drive behind this growth is its potential to replace vapor compression in many applications, primarily for improvements in efficiency (Engelbrecht, 2008). Magnetocaloric refrigeration relies on the magnetocaloric effect (MCE), which is typically observed as an adiabatic temperature change due to a change in magnetic field strength. Heat from the MCE can be harvested cyclically with a secondary heat transfer fluid in order to form a heat pump with a warm and a cold side. An interface between magnetocaloric material (MCM) and heat transfer fluid is known as an active magnetocaloric regenerator (AMR), and it often takes form as a fluidized packed bed of magnetocaloric particles. Many reviews summarize the operating principles as well as details of constructed machines using regenerative cycles (Yu, et al., 2010; Gomez, et al., 2013; Kitanovski, et al., 2014). The simplified AMR cycle as described by Brown (1976) consists of four segments:

1. Adiabatic magnetization; MCM temperature raises to high level.
2. Constant magnetization heat transfer; fluid is displaced. Fluid enters from the cold side, and heated fluid exits the hot-side.
3. Adiabatic demagnetization; MCM temperature falls to lower level than step 1.
4. Constant magnetization heat transfer; fluid is displaced in the opposite direction. Ambient temperature fluid enters from the hot side, and cooled fluid exits the cold side.

Modeling such a cycle is relatively straight forward fundamentally. A one dimensional model consists of two side-by-side arrays, fluid and MCM. MCM experiences a change in temperature or thermal energy on magnetization, the magnitude of which is determined by measured magnetocaloric properties. During all parts of the cycle heat is being transferred between fluid and solid radially, as well as between fluid and fluid axially. In addition mass transfer occurs axially between fluid nodes during flow. Any difference in outgoing versus incoming fluid temperature on the ends of the AMR is energy exchange with the environment. In the case of refrigeration, the cold side load is of primary concern, and represents a primary model output. Models such as this exist from multiple sources (Engelbrecht, 2008; Roudaut, et al., 2011; Aprea and Maiorino, 2010; Li, et al., 2011; Ivan, 2012; Risser, et al., 2013; Tagliafico, et al., 2013; Govindaraju, et al., 2014; Schroeder and Brehob, 2016). The main differences are

numerical schemes, additional modeled losses and effects, specific input and output parameters, and specific correlations for model physics. Correlation selection is critical for accurate results, and must be reconsidered for each flow regime and regenerator form. For packed beds many correlations exist relating Reynolds number (Re) and Prandtl number (Pr) to heat transfer coefficient between interstitial fluid and MCM. One of the more popularly used heat transfer correlations, by (Wakao et al., 1979), is listed as equation (1).

$$Nu = 2 + 1.1\, Re^{0.6}\, Pr^{1/3}. \quad (1)$$

Equation (1) is representative of the general form of most correlations, having an optional constant followed by Reynolds and Prandtl numbers raised to powers (Denton, et al., 1963; Gunn, 1978; Kunii and Levenspeil, 1969; Whitaker, 1972). What this also has in common with other correlations is that the confidence interval gets very large as Reynolds number approaches zero due to the nature of the experiments used (Wakao and Kagei, 1982). In the past this has not been an issue because technology hasn't relied very heavily on heat transfer between stagnant interstitial fluid and a packed bed. For magnetocaloric refrigeration, this case covers the entirety of cycle segments one and three, and therefore must be further explored. It seems that this case could be covered by correlations of natural convection, but they are valid only when strong convection currents exist in steady state. In the current work, transient heating occurs from all directions within each interstitial void between particles. Because of the small length scale and the transient nature of the process, it will be assumed that no significant convective currents are formed, as they require time to build momentum (Schroeder, 2014). It is the objective of this paper to provide an experimentally validated mathematical estimate of transient heat transfer between magnetocaloric particles and stagnant interstitial fluid with the assumption of pure conduction.

2. MATHEMATICAL MODEL

A very basic mathematical model can be developed to calculate heat transfer coefficient from material properties and geometry when pure conduction is assumed. In order to simplify the problem a two lumped mass system is modeled. The lumped masses considered are the two phases contained in the regenerator, solid and fluid. The average internal resistance of each phase will be used in series to calculate a total resistance. All temperatures used are bulk averages of either phase. In order to calculate thermal resistance a representative conduction length is needed for each phase. One approach, taken by (Engelbrecht, 2008) is to solve for the internal temperature gradient by assuming even internal generation. With this information internal particle thermal resistance can be calculated as a function of Biot number. The equivalent solid characteristic length for a sphere using this method is $1/10^{th}$ the particle diameter. Although realistic for the spherical case, this method again neglects irregular geometry. A more general definition of characteristic length (Incropera, et al., 2007) is volume per unit surface area. Given the irregular nature of the particles being studied, a variable is needed to adjust this ratio from known calculable geometric shapes. Sphericity is defined as the ratio of surface areas between a spherical particle and an irregular particle of equivalent volume (Wadell, 1935). A sphericity of one indicates a perfect sphere, and sphericity drops from there as irregularity increases. Characteristic length for solid non-spherical particles and interstitial fluid are given by equations (2) and (3) respectively.

$$L_{cs} = \frac{D_p \theta}{6} \qquad L_{cf} = \frac{D_p \theta}{6} \frac{\varepsilon}{(1-\varepsilon)} \quad (2), (3)$$

where L_{cf} is fluid phase characteristic length, L_{cs} is MCM characteristic length, D_p is particle diameter, θ is sphericity, and ε is regenerator void or fluid fraction. Taking the series thermal resistance of both phases results in equation (4).

$$U = \frac{1}{\left(\frac{D_p\, \theta}{6\, k_s} + \frac{D_p\, \theta\, \varepsilon}{6\,(1-\varepsilon)\, k_f}\right)} \quad (4)$$

where k_s is solid material thermal conductivity, and k_f is fluid material thermal conductivity. Heat transfer area per unit volume of regenerator is found by equation (5).

$$A_{hx} = \frac{6(1-\varepsilon)}{D_p \theta} \tag{5}$$

An explicit calculation is available for the presented two mass system, and it takes the form of equations (6) and (7) for fluid and solid phase temperatures with respect to time.

$$T_f(t) = T_\infty + \left(T_{if} - T_\infty\right)\exp\left(\frac{-t}{\tau_c}\right) \tag{6}$$

$$T_s(t) = T_\infty + \left(T_{is} - T_\infty\right)\exp\left(\frac{-t}{\tau_c}\right) \tag{7}$$

where T_∞ is equilibrium temperature, T_s is solid temperature, T_f is fluid temperature, t is time, and a subscript of i indicates initial state. The time constant for the system is given by equation (8).

$$\tau_c = \frac{1}{UA_{hx}} \frac{\varepsilon(\rho C_p)_f (1-\varepsilon)(\rho C_p)_s}{\left(\varepsilon(\rho C_p)_f + (1-\varepsilon)(\rho C_p)_s\right)} \tag{8}$$

where subscripts of s and f indicate solid and fluid phases respectively, C is specific heat, and ρ is the density. A derivation for equation 8 can be found in (Schroeder, 2014).

3. RESULTS

Two materials were used for model validation, La-Fe-Co-Si-H and Mn-Fe-P-As. Specific alloys of each were chosen that have a Curie temperature of approximately 75F. La-Fe-Co-Si-H has a thermal conductivity of about 8 W/mK (Legait, et al., 2014) (Liu, et al., 2012), while the Mn-Fe-P-As material thermal conductivity is about 2.5 W/mK (Fujieda, et al., 2004). Material densities are 7150 kg/m^3 (Legait, et al., 2014) and 6200 kg/m^3 (Brück, at al., 2013) for La-Fe-Co-Si-H and Mn-Fe-P-As respectively. Heat capacity is largely temperature dependent and was averaged across the small test temperature span to obtain a constant value to use in the basic model.

3.1 Measurements of Particle Sphericity

A pre-experiment pioneered by (Ergun, 1952) was performed on each material to obtain the average particle sphericity, as both materials are irregular in shape. Pressure drop across packed bed regenerators under steady flow was measured and compared to a fitted version of the Ergun equation (Ergun and Orning, 1949) shown as equation (9).

$$\Delta P = L_{bed}\left(A\frac{(1-\varepsilon)^2}{\varepsilon^3}\frac{\mu_f}{D_p^2}v_{sf} + B\frac{(1-\varepsilon)}{\varepsilon^3}\frac{\rho_f}{D_p}v_{sf}^2\right) \tag{9}$$

where v_{sf} is superficial velocity, μ_f is fluid viscosity, and A and B are viscous and inertial coefficients to be determined experimentally. A full factorial test matrix was run using spherical stainless steel particles to determine coefficients A and B for equation (9). Bed lengths used for these tests were 36.6, 86.4, and 317.5 mm, and the particle diameters were 363 and 635 μm. Void fraction was measured by weight at 0.36. Coefficients A and B from the baseline spherical cases were fitted using least squares regression, and were found to be 180 and 1.8 for the viscous and inertial terms respectively. Sphericity was implemented into the equation (9), as seen in (Ozahi, et al., 2008), resulting in an equation for pressure drop across irregular or spherical packed particle beds, given in equation (10).

$$\Delta P = L_{bed}\left(180\frac{(1-\varepsilon)^2}{\theta^2\varepsilon^3}\frac{\mu_f}{D_p^2}v_{sf} + 1.8\frac{(1-\varepsilon)}{\theta\varepsilon^3}\frac{\rho_f}{D_p}v_{sf}^2\right) \tag{10}$$

For irregular particle tests, bed lengths were 35.6 and 94 mm and particle diameters were 300-425, 425-600, and 1000-1400 μm. Measured void fraction was 0.42, again by weight. Pressure drop for the remaining test cases

utilizing irregular particles was used to fit sphericity values in equation (10). Particles of like material were assumed to have equal sphericity regardless of particle size. Sphericity was found to be 0.40 and 0.75 for La-Fe-Co-Si-H and Mn-Fe-P-As respectively with standard deviation of error being 8.6%.

3.2 Measurements of Heat Transfer Rate

In order to determine the heat transfer rate between stagnant fluid and the packed MCM a new approach was taken. Fluid was extracted from the end of the regenerator at different times after applying a magnetic field to the MCM. This period of time will be referred to as the dwell time. Extracted fluid temperature as a function of time was measured and compared to fluid temperature after a very long dwell period, representing the thermal equilibrium point of the solid-fluid matrix. By normalizing temperature in this way the thermal lag of the measurement system and the exact MCE magnitude are not needed. The fluid velocity and magnetic field state for the entirety of one test is shown in figure 1.

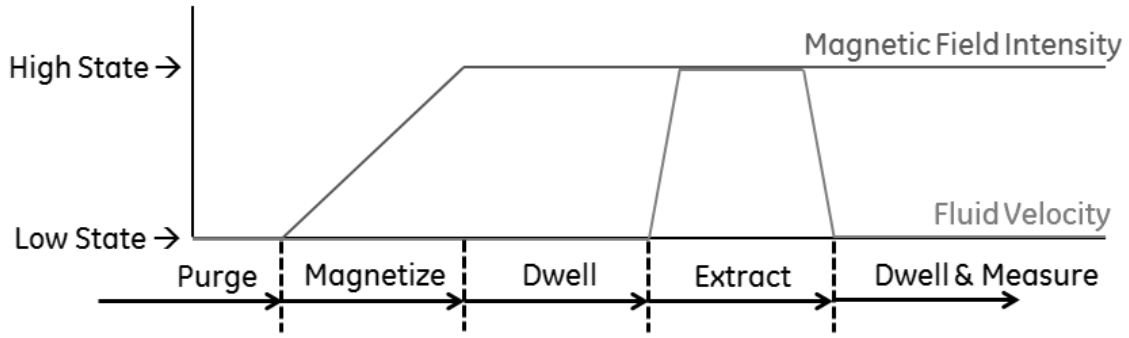

Figure 1: Test profiles for magnetic field and fluid velocity.

First a long purge period soaks all components at a constant temperature. Then, in rapid succession, the magnetic field is applied, the set dwell period is observed, a slug of fluid is extracted, and fluid temperature is measured during a second dwell period. Details of the experimental magnetic and hydraulic systems can be found in detail in (Benedict, et al., 2016). Fiber optic temperature sensors were used to measure extracted fluid temperature, as they have extremely low thermal mass. In order to fully magnetize the material, the outer Halbach cylinder must be accelerated and stopped 180 degrees from its starting position. The minimum time to accomplish this is approximately 0.1 s, and is determined by rotational inertia of the magnetic array and motor torque. This time represents the fastest possible magnetization time for this machine, and is on the same order of magnitude as the expected time constants for heat transfer. This means that most of the temperature profile measurements must be made on the latter half of the transition to ambient. Deionized water, ethylene glycol, and a 50-50 mix were used as working fluids. The fluid density, thermal conductivity, and heat capacity for all three fluids are shown in table 1.

Table 1: Test fluid properties.

Density kg/m^3	Thermal Conductivity W/mK	Heat Capacity J/kgK
981	0.58	4200
1045	0.42	3339
1110	0.26	2200

Particles sizes range from 300 to 1000 μm, but the smallest tested size was determined by the measurement system limitations. The smallest particles exchange heat too rapidly to be measured by the fixture. In these cases the temperatures of the fluid and solid have approached equilibrium during the magnetization time. This limit in measurability corresponds to a limit in practicality of a dwell period. With such rapid heat transfer occurring, fluid temperature can be approximated to be the same as material temperature in a model with little error. The test matrix contains two magnetocaloric materials, three fluids, and a maximum of three particle diameters for each material, shown in table 2.

Table 2: Heat transfer test matrix showing properties of fluid and MCM.

	Magnetocaloric Material (MCM)						Working Fluid		
Run	Material	Mean particle m	Sphericity	Density kg/m^3	Thermal conductivity W/mK	Heat capacity J/kgK	Density kg/m^3	Thermal conducti W/mK	Heat capacity J/kgK
1	Mn-Fe-P-As	0.0009	0.75	6300	2.5	900	981	0.58	4200
2	Mn-Fe-P-As	0.0009	0.75	6300	2.5	900	1045	0.42	3339
3	Mn-Fe-P-As	0.0009	0.75	6300	2.5	900	1110	0.26	2200
4	Mn-Fe-P-As	0.0007	0.75	6300	2.5	900	981	0.58	4200
5	Mn-Fe-P-As	0.0007	0.75	6300	2.5	900	1045	0.42	3339
6	Mn-Fe-P-As	0.0007	0.75	6300	2.5	900	1110	0.26	2200
7	Mn-Fe-P-As	0.0005	0.75	6300	2.5	900	981	0.58	4200
8	Mn-Fe-P-As	0.0005	0.75	6300	2.5	900	1045	0.42	3339
9	Mn-Fe-P-As	0.0005	0.75	6300	2.5	900	1110	0.26	2200
10	La-Fe-Co-Si-H	0.0011	0.4	7150	8	900	981	0.58	4200
11	La-Fe-Co-Si-H	0.0011	0.4	7150	8	900	1045	0.42	3339
12	La-Fe-Co-Si-H	0.0011	0.4	7150	8	900	1110	0.26	2200
13	La-Fe-Co-Si-H	0.0008	0.4	7150	8	900	981	0.58	4200
14	La-Fe-Co-Si-H	0.0008	0.4	7150	8	900	1045	0.42	3339
15	La-Fe-Co-Si-H	0.0008	0.4	7150	8	900	1110	0.26	2200
16	La-Fe-Co-Si-H	0.0005	0.4	7150	8	900	981	0.58	4200
17	La-Fe-Co-Si-H	0.0005	0.4	7150	8	900	1045	0.42	3339
18	La-Fe-Co-Si-H	0.0005	0.4	7150	8	900	1110	0.26	2200

The system thermal response is shown in figure 2. These are all measurements of a small fluid volume which has reached equilibrium temperature prior to extraction. This means the fluid leaving the regenerator is at a constant temperature.

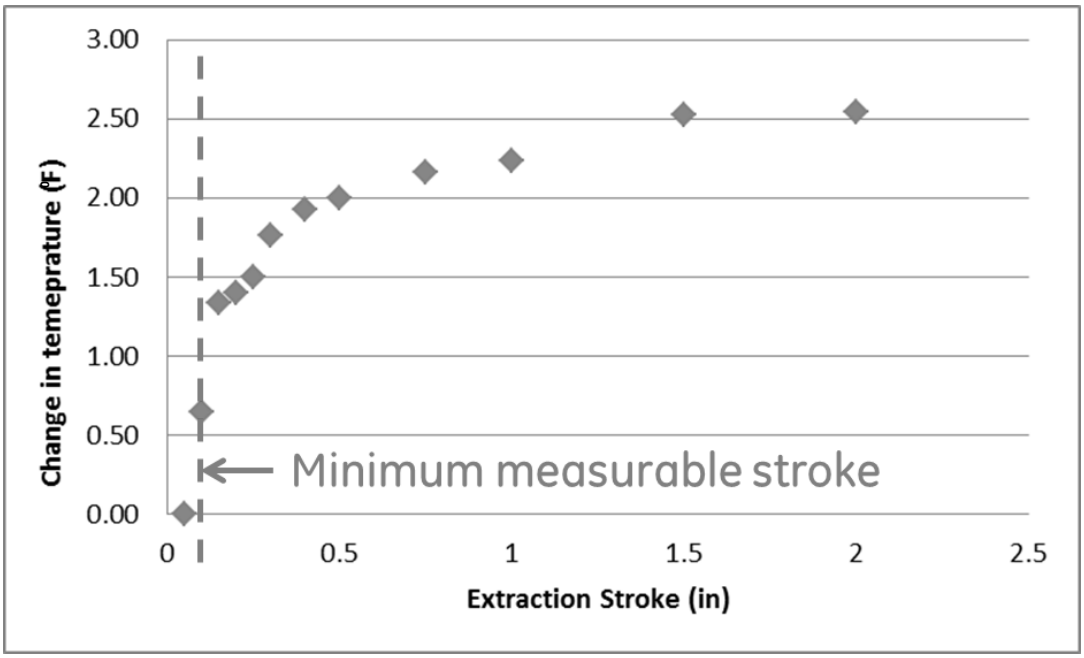

Figure 2: System thermal response for various stroke lengths with constant fluid temperature.

The relationship is approximately exponential, and varies with extraction velocity and working fluid composition. This particular case was performed with pure water, using a superficial regenerator velocity of 0.05 m/s. As the stroke increases, so does the measured change in temperature. Longer strokes at constant velocity provide more and more contact time, bringing the observed temperature closer and closer to true outgoing fluid temperature. This also illustrates the stroke required to capture the first fluid to exit the regenerator. The time constant of the system response can be used as a transfer function to translate a measured temperature change at minimum extraction stroke

to an actual fluid temperature leaving the regenerator. A total of three points must be run for each test case. For the first two points, the minimum stroke length and long stroke length equilibrium points are used to determine the measurement system time constant under the current conditions, shown in equation (11).

$$\tau_{c\,sys} = -\frac{t_{\underset{stroke}{min}}}{\ln\left(\frac{\Delta T_{\infty\,min}}{\Delta T_{\infty\,max}}\right)} \tag{11}$$

where $\tau_{c\,sys}$ is measurement system time constant for the specific fluid type and flow rate, $t_{\underset{stroke}{min}}$ is time required to move the minimum measureable stroke distance, $\Delta T_{\infty\,min}$ is measured temperature change using a long dwell period and the minimum stroke, and $\Delta T_{\infty\,max}$ is measured temperature change using a long dwell period and the longest stroke. For the third point, the actual test point is run and normalized to the equilibrium long stroke point. The previously determined system time constant is applied to the measurement to calculate actual fluid temperature at the end of the dwell period using equation (12).

$$\Delta T_{\underset{normalized}{f\,projected}} = \frac{\Delta T_{\underset{normalized}{f\,measured}}}{\exp\left(-\frac{t_{\underset{stroke}{min}}}{\tau_{c\,sys}}\right)} \tag{12}$$

where $\Delta T_{\underset{normalized}{f\,projected}}$ is normalized fluid outlet temperature, projected from the measured point and $\Delta T_{\underset{normalized}{f\,measured}}$ is normalized fluid measured temperature. The reason for normalizing the temperature response is to maintain comparability between tests, regardless of magnitude of magnetocaloric effect. This method of measurement also requires the approximation of constant outlet temperature. Because the measured fluid is the first fluid to leave the regenerator, a near constant temperature should hold true. If a measurement were taken of fluid deeper inside the regenerator, this would no longer hold true. Running the test for several different dwell times yields a profile of points, as is shown in figure 3.

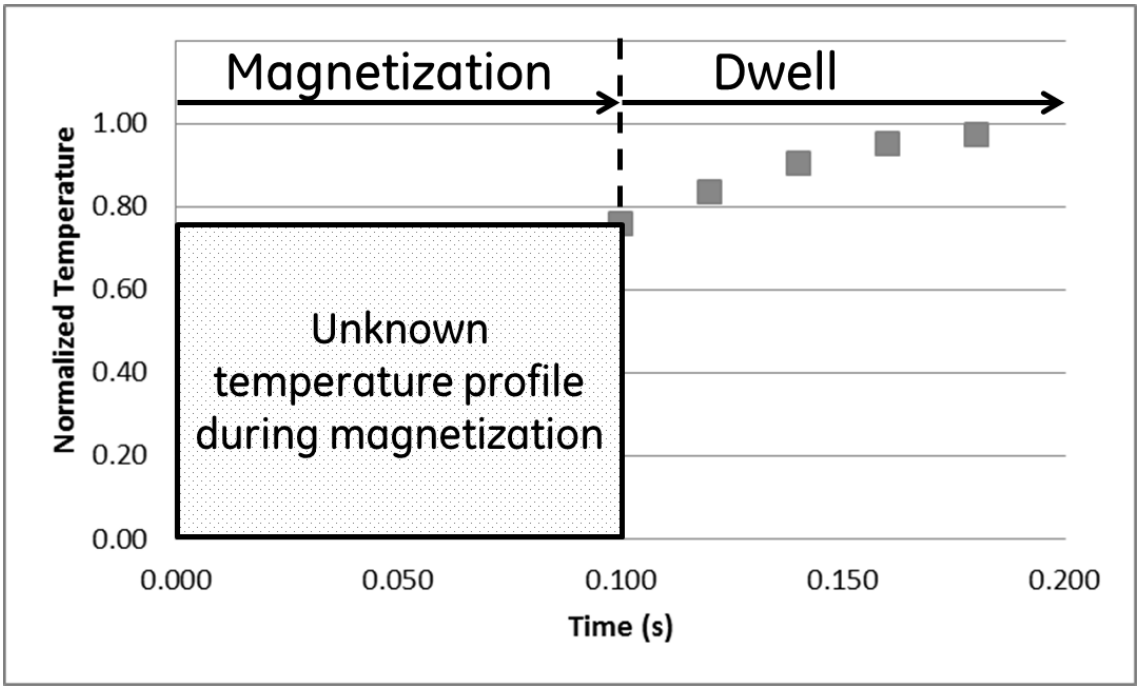

Figure 3: Example of measured temperature with respect to dwell time.

The time scale on this set of results includes magnetization time. For this particular case 75% of heat was transferred during magnetization. The remainder of heat was transferred within the following 0.1 s. To account for run to run variability, multiple sets of points were run and averaged for each test case until the average output converged. The final step is to translate the observed average time constant into a U value (equation 8). Each calculated U value comes from at least five temperature profiles, with at least five points each (figure 3). Of the possible 18 test cases, only nine were measurable using the equipment. The rest of the material transferred heat too

quickly to get an accurate measurement using this method. This means that the resulting correlation is the result of just over 300 dwell measurements in total. The average measured UA values per unit regenerator volume are plotted for each of the nine test cases in figure 4.

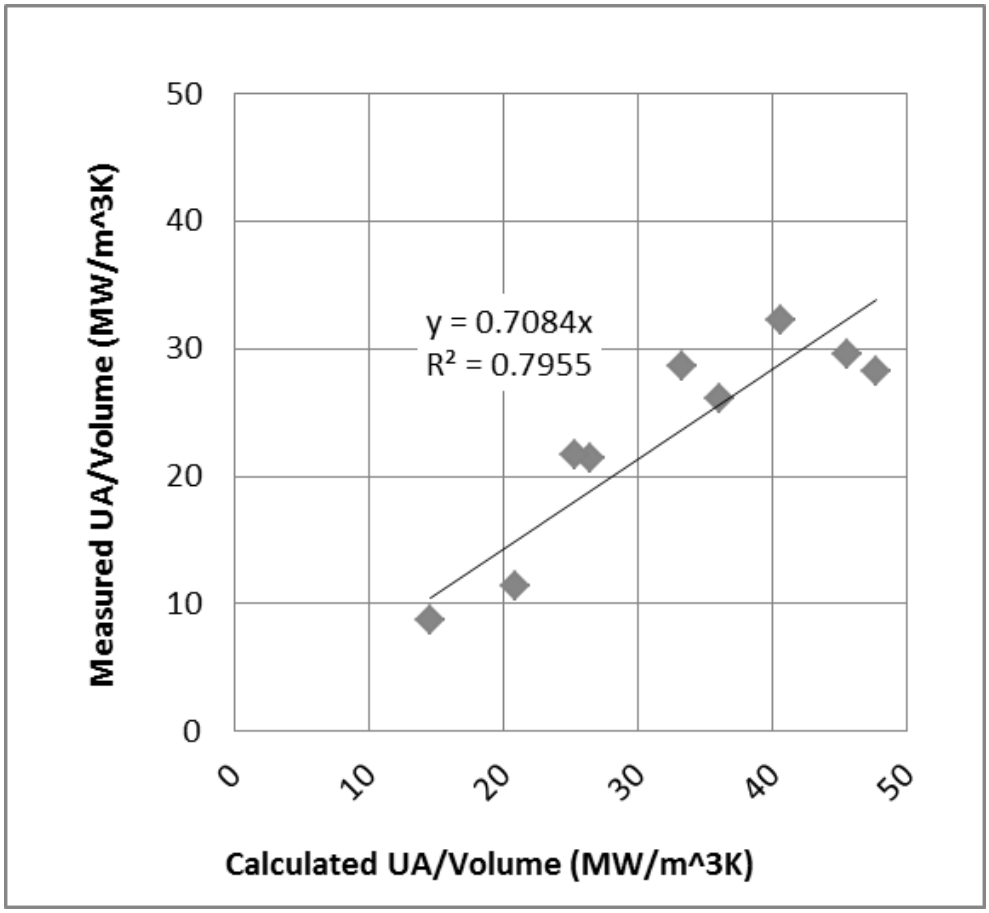

Figure 4: Fit of measured values to equation 12 predictions.

The R-squared value for the correlation is about 0.8, suggesting that the model is capturing the critical variables and effects. However, the slope of the fit curve shows that the measured values are 30 % lower than the calculated values using the model presented. By applying a multiplied correction factor of 0.70 to the output of the analytical model, maximum model error becomes 20 %. The final correlation for heat transfer coefficient is given in equation (13).

$$U = \frac{0.70}{\left(\frac{L_{cs}}{k_s} + \frac{L_{cf}}{k_f}\right)} = \frac{0.70}{\left(\frac{D_p\,\theta}{6\,k_s} + \frac{D_p\,\theta\,\varepsilon}{6\,(1-\varepsilon)\,k_f}\right)} \tag{13}$$

where θ is sphericity (0 to 1), D_p is mean particle diameter, ε is void or fluid fraction in regenerator packing, k_s is solid material conductivity, and k_f is fluid material conductivity. As a point of reference the equivalent fluid characteristic length, given by equation (13), and using typical void fraction and spherical particles is shown in equation (14).

$$L_{cf} = \frac{D_{p\theta}}{6}\frac{\varepsilon}{(1-\varepsilon)}\frac{1}{0.70} = \frac{D_p}{5.8} \tag{14}$$

The conductive heat transfer coefficient can be superimposed with flow correlations in order to create a continuous Nusselt number function. For instance, the constant with the (Wakao, et al., 1979) correlation found in equation (1) can be modified to form

$$Nu = 0.70\ \frac{6\,(1-\varepsilon)}{\theta\ \varepsilon} + 1.1\ Re^{0.6}\ Pr^{1/3} \quad (15)$$

4. SUMMARY

In summary, a model was created to calculate average heat transfer coefficient from geometric parameters and material properties. This model relies on a generic characteristic length calculation for both the fluid and solid phases within the regenerator. A pre-experiment was performed to measure particle sphericity. The results allowed for an independent measurement of heat transfer area. Then an experiment was carried out to measure the fluid temperature over time after magnetization. Parameters such as particle diameter, particle thermal conductivity, and fluid thermal conductivity were varied to assess the modeled heat transfer coefficient. The experiment led to a correction factor being added to the basic model. Finally, the result was used to modify an existing flow correlation to create an improved continuous Nusselt number correlation. The model was validated for a random close pack of irregular particles from 0.4-0.75 sphericity, but the model should be useful for an even larger range of cases.

BIBLIOGRAPHY

Aprea, C., and A. Maiorino. "A flexible numerical model to study an active magnetic refrigerator for near room temperature applications." *Appl. Energy 87*, 2010: 2690-2698.

Benedict, M. A., S. A. Sherif, D. G. Beers, and M. G. Schroeder. "Design and Performance of a Novel magnetocaloric Heat Pump." *ASHRAE Science and Technology for the Built Environment*, 2016.

Brown, G.V. "Magnetic heat pumping near room temperature." *Journal of Applied Physics* 47 (1976): 3673-3680.

Brück, E. H., N. H. Van Dijk, and Z. Q. Ou. "Magnetic structure and phase formation of magnetocaloric Mn-Fe-P-X compounds." *Uitgeverij BOXPress, 's-Hertogenbosch*, 2013.

Churchill, S. W. "A compreshensive correlation equation for laminar, assisted, forced, and free convection." *Aiche Journal* 23, no. 1 (1977): 10-16.

Denton, W. H., C. H. Robinson, R. S. Tibbs, and United Kingdom Atomic Energy Authority. "The heat transfer and pressure loss in fluid flow through randomly packed spheres." *Harwell, Berkshire, England: Scientific Administration Office, Atomic Eenrgy Research Establishment*, 1963.

Engelbrecht, K. *A Numerical Model of an Active Magnetic Regenerator Refrigerator with Experimental Validation (Ph.D. thesis).* USA: University of Wisconsin-Madison, 2008.

Ergun, S. "Determination of Geometric Surface Area of Crushed Porous Solids." *Analytical Chemistry* 2, no. 24 (1952): 388-393.

Ergun, S., and A. A. Orning. "Fluid Flow through Randomly Packed Columns and Fluidized Beds." *Industrial & Engineering Chemistry* 41, no. 6 (1949): 1179-1184.

Fujieda, S., Y. Hasegawa, A. Fujita, and K. Fukamichi. "Thermal transport properties of magnetic refrigerants La(Fex~Si1~-~x~)1~3~ and their hydrides, and Gd5~Si2~Ge2~ and MnAs." *Journal of Applied Physics* 95 (2004): 2429-2431.

Globe, S., and D. Dropkin. *Journal of Heat Transfer* 81C, no. 24 (1959).

Gomez, J.R., R.F. Garcia, J.C. Carril, and M.R. Gomez. "A review of room temperature linear reciprocating magnetic refrigerators." *Renewable and Sustainable Energy Reviews*, 2013: 1-12.

Govindaraju, V.R., D.M. Vilathgamuwa, and R.V. Ramanujan. "Modelling of a magnetocaloric system for cooling in the kilowatt range." *Int. J. Refrigeration*, 2014: 143-153.

Gschneider Jr., K.A., and V.K. Pecharsky. "Thirty years of near room temperature magnetic cooling: where we are today and future prospects." *Int.l J. of Refrigeration 31*, 2008: 945-961.

Gunn, D. J. "Transfer of heat or mass to particles in fixed and fluidized beds." *International Journal of Heat and Mass Transfer* 21, no. 4 (1978): 467-476.

Incropera, F. P., D.P. Dewitt, T.L. Bergman, and A.S. Lavine. *Introduction to Heat Transfer.* Hoboken: Wiley, 2007.

Ivan, M.B. *Assessment of Magnetic Cooling for Domestic Applications (Master of Science thesis).* Sweden: KTH School of Industrial Engineering and Management, 2012.

Kitanovski, A., J. Tusek, T. Urban, U. Plaznik, M. Ozbolt, and A. Poredos. *Magnetocaloric Energy Conversion: From Theory to Applications (Green Energy and Technology).* New York: Springer, 2014.

Kunii, D., and O. Levenspeil. *Fluidization Engineering.* New York, New York: Wiley, 1969.

Legait, U., F. Guillou, A. Kedous-Lebouc, V. Hardy, and M. Almanza. "An experimental comparison of four magnetocaloric regenerators using three different materials." *International Journal of Refrigeration* 37 (2014): 147-155.

Li, J., T. Numazawa, H. Nakagome, and K. Matsumoto. "Numerical modeling on a reciprocating active magnetic regenerator refrigeration in room temperature." *Cryogenics 51*, 2011: 347-352.

Liu, J., J. D. Moore, K. P. Skokov, K. Lowe, A. Barcza, and M. Katter. "Magnetic Materials for Energy. (September 01, 2012). Exploring La(Fe,Si)"1"3-based magnetic refrigerants towards application." *Scriptia Materialia* 67, no. 6 (2012): 584-589.

Ozahi, E., M. Y. Gundogdu, and M. O. Carpinlioglu. "A Modification on Ergun's Correlation for Use in Cylindrical Packed Beds With Non-spherical Particles." *Advanced Powder Technology* 19, no. 4 (2008): 369-381.

Risser, M., C. Vasile, C. Muller, and A. Noume. "Improvement and application of a numerical model for optimizing the design of magnetic refrigerators." *Int. J. Refrigeration 36*, 2013: 950-957.

Roudaut, J., A. Kedous-Lebouc, J.P. Yonnet, and C. Muller. "Numerical analysis of an active magnetic regenerator." *Int. J. Refrigeration 34*, 2011: 1797-1804.

Schroeder, Michael G. "Transient Heat Transfer Between a Magnetocaloric Packed Particle Bed and Stagnant Interstitial Fluid." *University of Louisville Mechanical Engineering Department*, 2014.

Schroeder, Michael G., and Ellen Brehob. "A Flexible Numerical Model of a Multistage Active Magnetocaloric Regenerator." *International Journal of Refrigeration*, 2016.

Tagliafico, G., F. Scarpa, and L.A. Tagliafico. "A dimensionless description of active magnetic regenerators to compare their performance and to simplify their optimization." *Int. J. Refrigeration 36*, 2013: 941-949.

Wadell, H. "Volume, Shape, and Roundness of Quartz Particles." *The Journal of Geology* 43, no. 3 (1935): 250-280.

Wakao, N., and S. Kagei. *Heat and Mass Transfer in Packed Beds.* New York: Gordon and Breach Science Publishers, 1982.

Wakao, N., S. Kaguei, and T. Funazkri. "Effect of fluid dispersion coefficients on particle-to-fluid heat transfer coefficients in packed beds:Correlation of nusselt numbers." *Chemical Engineering Science, 34*, no. 3 (1979): 325-336.

Whitaker, S. "Forced convection heat transfer correlations for flow in pipes, past flat plates, single cylinders, single spheres, and for flow in packed beds and tube bundles." *Aiche Journal* 18, no. 2 (1972): 361-371.

Yu, B., M. Liu, P.W. Egolf, and A. Kitanovski. "A review of magnetic refrigeration and heat pump prototypes built before the year 2010." *Int. J. Refrigeration 33*, 2010: 1029-1060.